11th World Congress on Structural and Multidisciplinary Optimisation
07th -12th, June 2015, Sydney Australia

Fatigue Sensitivity Analysis of Offshore Wind Turbine Structures

Kok-Hon Chew[1], Michael Muskulus[2], Srikanth Narasimalu[3], Kang Tai[4], E.Y.K. Ng[5]

[1]School of Mechanical and Aerospace Engineering, Nanyang Technological University, Singapore, chew0272@e.ntu.edu.sg
[2]Department of Civil and Transport Engineering, Norwegian University of Science and Technology, Trondheim, Norway, michael.muskulus@ntnu.no
[3]Energy Research Institute @ NTU, Nanyang Technological University, Singapore, nsrikanth@ntu.edu.sg
[4]School of Mechanical and Aerospace Engineering, Nanyang Technological University, Singapore, mktai@ntu.edu.sg
[5]School of Mechanical and Aerospace Engineering, Nanyang Technological University, Singapore, mykng@ntu.edu.sg

1. Abstract
Design optimization of offshore wind turbine structures is generally fatigue driven, yet the fatigue sensitivities with respect to design variables are commonly approximated using finite differences, leading to inefficiency and unreliable information. This paper presents analytical methods to calculate the gradients of fatigue damage and equivalent fatigue loads in both time and frequency domains, focusing on their use with the rainflow counting and Dirlik's methods, respectively, for implementation in the optimization of offshore wind turbine structures. Comparison studies against finite difference schemes, for simulated stress data experienced by the OC4 jacket substructure, show that the fatigue damage gradients were very sensitive to response sensitivities, while highlighting several key suggestions which could improve the numerical fatigue sensitivity analysis.
2. Keywords: Fatigue; sensitivity analysis; structural optimization; gradient-based; offshore wind.

3. Introduction
Fatigue assessment is critical in the design of offshore wind turbine structures, as the structures experience vibrations during operation, while subject to time-varying wind and wave loads [1]. When performing structural optimization, the gradients of fatigue damage with respect to design variables are valuable for an optimizer to determine the best direction for improvement [2]. A finite difference method is commonly employed to approximate the sensitivity information, since the method is easy to implement while the dynamic analysis of a wind turbine system generally requires specialized software which often cannot be modified or extended [2,3]. Nevertheless, the method can be inefficient and unreliable when it is used for design sensitivity analysis [4]. On the other hand, the analytical formulae for fatigue damage sensitivities cannot be evaluated readily. Various fatigue assessment techniques (e.g. in the time domain and by spectral methods) are available and the process to calculate stress range histograms or stress range probability density functions (PDF) requires one to go through the cycle counting or the Fourier transform, respectively. In this paper, methods to calculate the analytical fatigue damage gradients for both time and frequency domains are presented. Further studies are carried out to compare them against the finite difference schemes under consideration of various parameters, such as step sizes, time steps, joint configurations and stress concentration effects; and discuss their implications on the fatigue gradients estimation.

4. Fatigue assessment of offshore wind turbine structures
The general approach for fatigue assessment of offshore wind turbine structures is documented in [5,6,7]. Fig. 1 illustrates the procedure. Internal nominal stresses, in the form of time series which are recovered from system responses, are pre-multiplied with Stress Concentration Factors (SCF) and superimposed to obtain the Hot Spot Stresses (HSS). The SCF can be computed using empirical formulae as prescribed by Det Norske Veritas, given the joint class, geometry and dimensions [5]. As for the HSS, they are evaluated at eight different spots around the circumference of joint intersections, at both brace and leg sides.
The HSS output is variable in amplitudes; therefore post-processing is required to estimate the stress ranges before one can proceed to calculate the fatigue damage. This can be achieved either by using cycle counting or spectral techniques. ASTM's rainflow counting algorithm is a commonly used cycle counting method which identifies the stress ranges and associated number of cycles (half or full cycles) for the HSS time series by pairing the peaks and valleys in analogy with rain flowing down a pagoda roof [8]. Alternatively, the Dirlik's method obtains the stress range PDF from a spectrum. It assumes that the stress range PDF is a weighted combination of an exponential and two Rayleigh distributions; and is intended for both wide- and narrow-band processes [9]. The Dirlik's method is frequently used in conjunction with dynamic analysis performed in the frequency domain, where the power spectral density (PSD) of HSS is calculated using transfer functions. The individual stress ranges of the histogram or PDF are then compared against the S-N curves to determine the fatigue damage. By applying the Palmgren-Miner's rule, the damage for each stress range is summed up linearly, which gives the total accumulated damage.

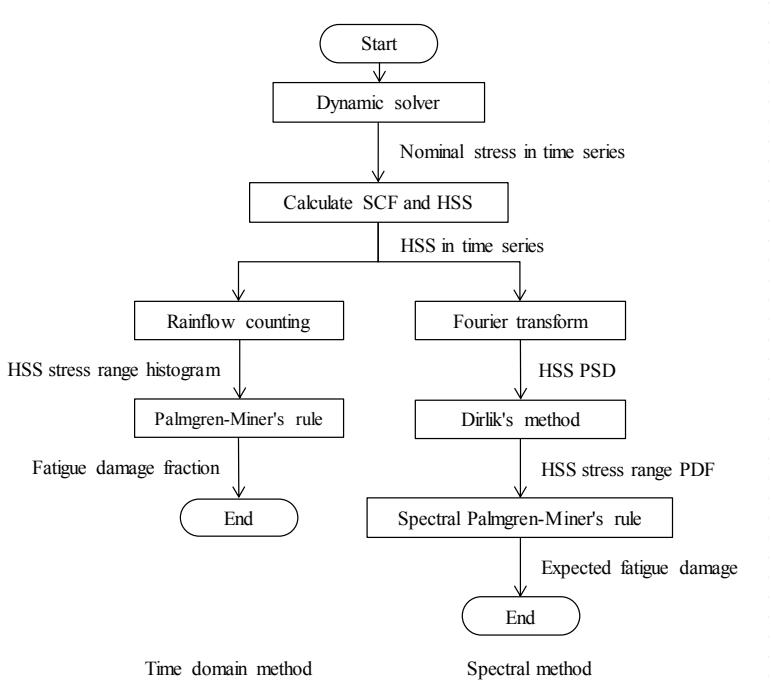

Figure 1: Procedure to calculate fatigue damage, either using time domain or spectral method

5. Methodology to calculate analytical fatigue gradients

The gradients of fatigue damage with respect to design variables were obtained analytically using the Direct Differentiation Method (DDM) [10]. The term 'fatigue damage' refers to the fraction of accumulated fatigue damage, with 0 meaning fatigue free and 1 signifying failure. This is also called fatigue utilization factors.

5.1 Time domain method

The gradients of fatigue damage D and equivalent fatigue loads EFL, using DDM, were given by Eqs. (1) and (2), respectively:

$$\nabla D = \sum_{i=1}^{I} \left[\frac{m n_i}{\bar{a}} \cdot \left(S_i\right)^{m-1} \cdot \frac{\mathrm{d}S_i}{\mathrm{d}\mathbf{b}} \right] \tag{1}$$

$$\nabla EFL = \frac{1}{mD} \cdot \left(\frac{\bar{a} D}{N} \right)^{\frac{1}{m}} \cdot \nabla D \tag{2}$$

where $\bar{a}$ = intercept of S-N curve with log N axis; m = negative inverse slope of the S-N curves; S_i = stress range of HSS [MPa]; n_i = number of stress cycles corresponding to S_i; and $\mathbf{b}$ = design variable vector. The S_i here referred to the individual stress ranges without binning, while n_i corresponded to either a half or full cycle. As such, the $\mathrm{d}n_i/\mathrm{d}\mathbf{b}$ term could be neglected in Eq. (1).

The derivative of stress range $\mathrm{d}S_i/\mathrm{d}\mathbf{b}$ was calculated by taking the difference of stress (in this case HSS) sensitivities $\mathrm{d}\sigma(t)/\mathrm{d}\mathbf{b}$ at $t = t_{i,1}$ and $t = t_{i,2}$, where $t_{i,1}$ and $t_{i,2}$ are the times of initial and reversal points for S_i, respectively, see Eq. (3). The $t_{i,1}$ and $t_{i,2}$ could be identified during the rainflow counting process.

$$\frac{\mathrm{d}S_i}{\mathrm{d}\mathbf{b}} = \begin{cases} \left.\dfrac{\mathrm{d}\sigma(t)}{\mathrm{d}\mathbf{b}}\right|_{t=t_{i,1}} - \left.\dfrac{\mathrm{d}\sigma(t)}{\mathrm{d}\mathbf{b}}\right|_{t=t_{i,2}} & \text{for } \sigma\left(t_{i,1}\right) > \sigma\left(t_{i,2}\right) \\ \left.\dfrac{\mathrm{d}\sigma(t)}{\mathrm{d}\mathbf{b}}\right|_{t=t_{i,2}} - \left.\dfrac{\mathrm{d}\sigma(t)}{\mathrm{d}\mathbf{b}}\right|_{t=t_{i,1}} & \text{for } \sigma\left(t_{i,2}\right) > \sigma\left(t_{i,1}\right) \end{cases} \tag{3}$$

3.2 Spectral method

The gradient of expected fatigue damage $E[D]$, by using DDM, could be written as Eq. (4):

$$\nabla E[D] = \frac{T}{\bar{a}} \cdot \left\{ \sum_{k=1}^{K} \left[S_k^m \cdot p(S_k) \cdot \Delta S_k \right] \cdot \frac{\mathrm{d}}{\mathrm{d}\mathbf{b}} E[P] + E[P] \cdot \sum_{k=1}^{K} \frac{\mathrm{d}}{\mathrm{d}\mathbf{b}} \left[S_k^m \cdot p(S_k) \cdot \Delta S_k \right] \right\} \tag{4}$$

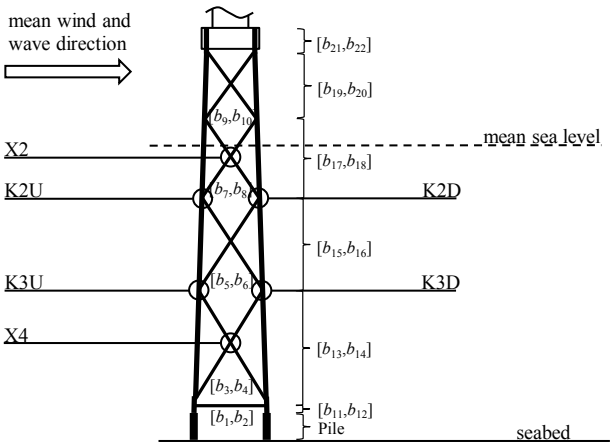

Figure 2: OC4 Jacket substructure model and locations identified for simulated HSS data output

where $p(S)$ = Dirlik's stress range PDF; T = total time [s]; and $E[P]$= expected number of peaks per unit time [s^{-1}]. The empirical distribution weight factors of $p(S)$ and $E[P]$ are governed by spectral moments m_n:

$$m_n = \sum_{l=1}^{L}\left[f_l^n \cdot P_s(f_l)\cdot \Delta f_l\right] \tag{5}$$

The PSD $P_s(f)$ was obtained by the Fourier transform of $\sigma(t)$. The Welch method (modified periodogram) with Hamming windows and overlaps was used in this study, as the taper reduces leakage from the spectral density near the large peaks in the spectrum [11]. The sensitivity of Welch's method was derived as:

$$\begin{aligned}
\frac{\mathrm{d}}{\mathrm{d}\mathbf{b}}P_s(f) &= \frac{4}{QJUF_s}\sum_{q=1}^{Q}\left[\mathrm{Re}\left(A_q(f)\right)\cdot\mathrm{Re}\left(A_q'(f)\right)+\mathrm{Im}\left(A_q(f)\right)\cdot\mathrm{Im}\left(A_q'(f)\right)\right]\\
\text{where } \mathrm{A}_q(f) &= \sum_{j=0}^{J-1}\left[\sigma_q(j)\cdot W(j)\cdot\exp\left(-2\pi ijf/J\right)\right]\\
\mathrm{A}_q'(f) &= \sum_{j=0}^{J-1}\left\{\frac{\mathrm{d}}{\mathrm{d}\mathbf{b}}\left[\sigma_q(j)\right]\cdot W(j)\cdot\exp\left(-2\pi ijf/J\right)\right\}\\
U &= \frac{1}{J}\sum_{j=0}^{J-1}W^2(j)
\end{aligned} \tag{6}$$

where Q = number of window segments; J = number of samples within the window; W = windowing function (e.g. Hamming); F_s = sampling frequency; and $i=\sqrt{-1}$. Note: Scaling factor of $1/J$ to be used for samples at zero frequency and Nyquist frequency. Comparably, the gradient of EFL for the spectral method was derived as:

$$\nabla EFL = \frac{1}{m}\cdot\left(\frac{\bar{a}\cdot E[D]}{E[N]}\right)^{\frac{1}{m}}\cdot\left(\frac{\nabla E[D]}{E[D]}-\frac{\nabla E[N]}{E[N]}\right) \tag{7}$$

The $E[N]$in Eq. (7), unlike $N=\sum n_i$ in Eq. (2), is a function of m_n and therefore varies with respect to $\mathbf{b}$.

6. Comparison of fatigue damage sensitivities

A comparison between analytical and numerical fatigue damage sensitivities was carried out on simulated stress data obtained from the numerical wind turbine model used within the Offshore Code Comparison Collaboration Continuation (OC4) Project. The model consists of the 5 MW wind turbine model developed by National Renewable Energy Laboratory, mounted on a support structure system that includes a tubular tower, a concrete transition piece and a jacket substructure [12,13]. The HSS were evaluated at six distinct locations. They are the middle K-joints facing upwind (K2U) and downwind (K2D), the bottom K-joints facing upwind (K3U) and downwind (K3D), the X-joints at 2nd bay (X2) and 4th bay (X4) from top (Fig. 2). The vector **b** consists of 22 design variables, i.e. $b_1 - b_{22}$, where the odd and even numbered variables represent the member diameters and thicknesses, respectively. The fatigue damage sensitivities were evaluated at initial jacket dimensions against the 4th bay brace diameter b_3, 4th bay brace thickness b_4, 4th bay leg diameter b_{13}, 4th bay leg thickness b_{14}, 2nd bay brace diameter b_7, 2nd bay brace thickness b_8, 2nd bay leg diameter b_{17} and 2nd bay leg thickness b_{18}.

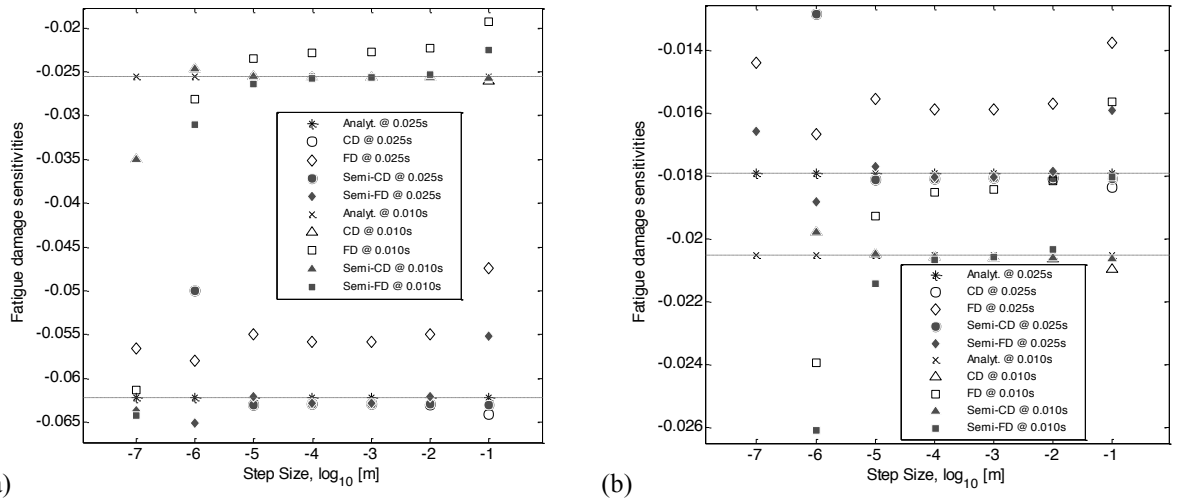

Figure 3: Comparison of fatigue damage sensitivities varying against design variable step sizes and time steps in the numerical sensitivity analysis, for (a) spectral and (b) time domain methods. Sensitivities were calculated against b_{13} at hot spot location 1 of K3U (leg side) joint.

6.1 Step sizes and time steps

Fig. 3 depicts the variation of fatigue damage sensitivities with respect to step sizes and time steps used in the sensitivity analysis. The design variables were perturbed in steps of tenfold increments from 10^{-7} to 10^{-1}, while two different time steps, 0.025 s and 0.010 s, were used. Both central difference (CD) and forward difference (FD) schemes followed different patterns, with each attaining minimum numerical errors at different step sizes. The 'optimal' step sizes also varied for different joint and hot spot locations (not shown here), resulting in difficulties to determine a 'good' step size to be used in the overall design sensitivity analysis. The numerical errors consist of truncation and condition errors, which are positively and inversely proportional to the step sizes, respectively. The CD generally yielded smaller numerical errors as compared with the FD due to a higher order of approximation. However, in some cases, the CD could be more erroneous (Fig. 4). Similarly, the finite difference approximations improved when smaller time steps were used. The analytical solutions for fatigue damage sensitivities between the time domain and spectral methods came closer when a smaller time step was implemented. The spectral method was more sensitive to the time step change, since the method is based on the Fourier transform which is more susceptible to the quality of input signals. Besides, the semi-finite difference methods could help to enhance the numerical sensitivity analysis. In this method, the HSS sensitivities were estimated numerically using finite difference schemes while the final fatigue sensitivity analysis was performed using analytical formulations. The results of this approach matched well with the finite difference methods (Fig. 4). However, in some cases, they could avoid numerical artefacts, as shown for the FD in Fig. 3. The above mentioned findings have demonstrated the subtle characteristics of fatigue sensitivity analysis with regard to the response sensitivities. Therefore, it is imperative to make sure that the quality of response sensitivities is sufficient when calculating the numerical gradients for fatigue damage. Often the analytical solutions are not available for the response sensitivities due to software constraints. In such case, the semi-finite difference approach is suggested.

6.2 Joint locations and hot spot locations

Fig. 4 summarizes the fatigue damage sensitivities calculated using the analytical, finite difference and semi-finite difference methods at various joint and hot spot locations. The last two were taken at step sizes which resulted in the smallest numerical errors. The percentage errors of numerical sensitivities against the analytical solutions (1st bars) were listed above and below the respective bars, for the time domain and spectral methods.

In Fig. 4(a), the fatigue damage sensitivities at specific joint locations are shown to be localized, i.e. to be influenced most by the design variables which the joint was directly connected to. The finite difference schemes also gave smaller errors when evaluating fatigue sensitivities at locations where the design variable was directly connected to. On the contrary, the associated errors at joint locations where the design variables were not in connection with could reach values as high as 1700 percent or could be wrong in sign. Whereas Fig. 4(b) indicates that the fatigue damage sensitivities were distinct at various hot spot locations. Although the time domain and spectral methods differ in estimating the damage sensitivities (of which the accuracy depends on the quality of response sensitivities), the percentage errors of their finite difference counterparts were generally similar in scale.

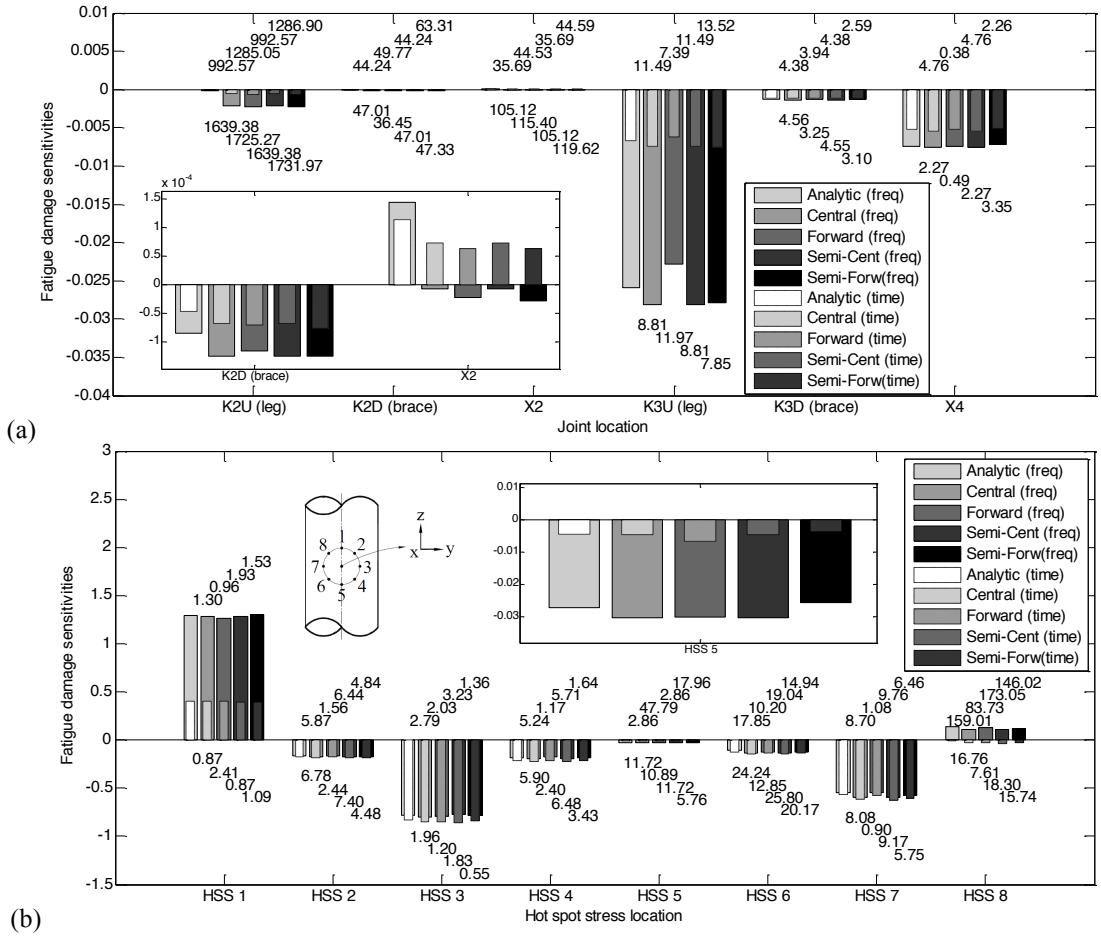

Figure 4: Comparison of fatigue damage sensitivities at various (a) joint locations and (b) hot spot locations. (a) Sensitivities were calculated against b_3 at hot spot location 1 for various joints and (b) Sensitivities were calculated against b_8 at K2U (leg side) for 8 hot spot locations using time domain ('time') and spectral ('freq') methods.

6.3 Stress concentration effects

So far all the fatigue damage sensitivities discussed earlier have considered the SCF variations against the design variables. However, since the empirical formulae to estimate the SCF are laborious to use, it raised the interest to investigate the contributions of SCF derivatives in the overall fatigue sensitivity analysis. HSS are geometric stresses that account for stress concentration effects occurring at the joint regions. The sensitivities depend on both the sensitivities of nominal stress as well as the sensitivities of SCF with respect to design variables. Fig. 5 shows the analytical fatigue damage sensitivities, performed with and without consideration of the SCF derivatives. The SCF were treated as constants in the latter case. Results indicate that the SCF derivatives exerted significant influences in the calculation, for all joint types. In some cases, the sensitivities could be inverted in sign. Therefore, it is important to include the SCF variations in the gradient assessment of fatigue damage, when HSS are used.

7. Conclusions

This paper presented analytical formulations to calculate the gradients of fatigue damage and equivalent fatigue loads, for both time domain and spectral methods. Detailed comparison studies using the stress data obtained from the numerical OC4 wind turbine model revealed that:

- Fatigue sensitivity analysis was very susceptible to the quality of response sensitivities. Several recommendations which could help improve the overall quality of numerical sensitivities include using sufficiently small step sizes when perturbing the design variables; implementing more robust time domain methods when evaluating the fatigue damage; or adopting the semi-finite difference methods.
- The fatigue damage sensitivities were localized, as they were affected most by the design variables in close proximity with the joints. The errors associated with fatigue damage sensitivities for joints which the design variables were not directly connected to, could be very high for the finite difference approximations.
- The derivatives of SCF exerted significant influences in determining the fatigue damage sensitivities. This should always be considered when the hot spot stress methodology is used for the fatigue assessment.

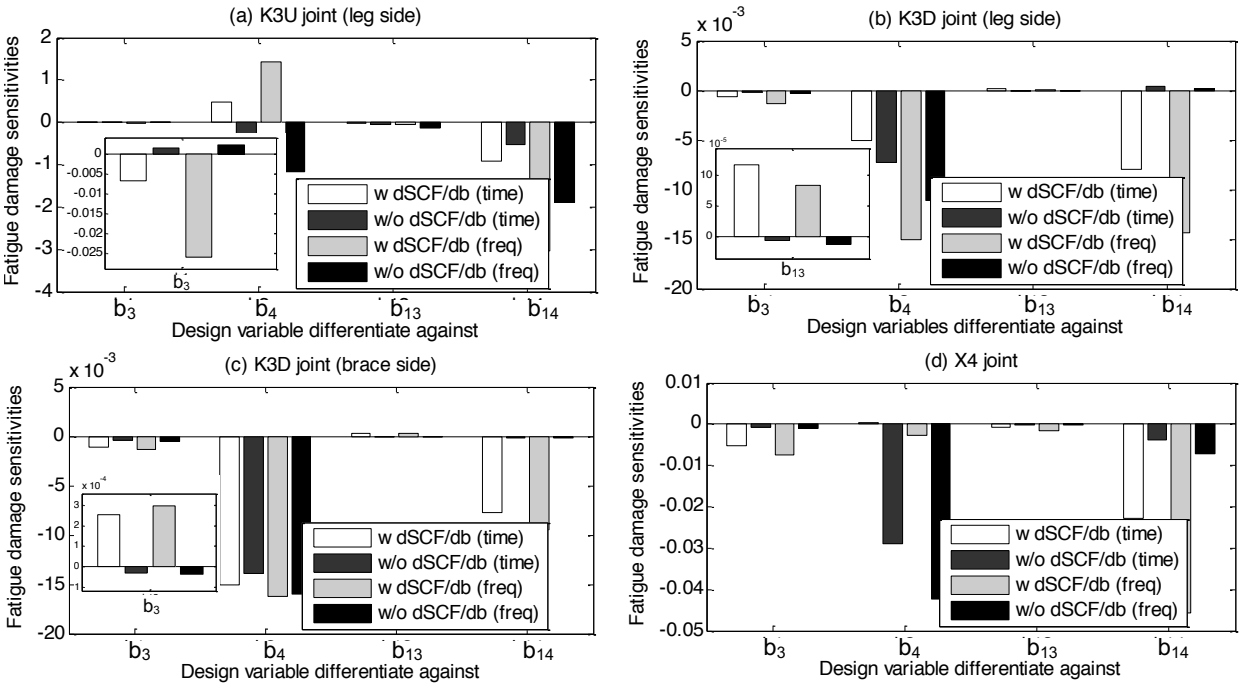

Figure 5: Comparison of analytical fatigue damage sensitivities with and without consideration of SCF derivative. Sensitivities are calculated against b_i at hot spot location 1 for various joints using time domain ('time') and spectral ('freq') methods.

8. Acknowledgements

The authors would like to thank the Singapore Economic Development Board (EDB) – DNVGL – Energy Research Institute @ NTU (ERI@N) Joint Industry PhD Program. Support from Norwegian Research Centre for Offshore Wind Technology (NOWITECH FME, Research Council of Norway, grant 193923) is acknowledged.

9. References

[1] F. Vorpahl, H. Schwarze, T. Fischer, M. Seidel and J. Jonkman, Offshore Wind Turbine Environment, Loads, Simulation, and Design, *WIREs Energy Environ*, 2, 548-570, 2013.

[2] M. Muskulus and S. Schafhirt, Design Optimization of Wind Turbine Support Structures – A Review, *Journal of Ocean and Wind Energy*, 1 (1), 12-22, 2014.

[3] D.A. Tortorelli and M. Panagiotis, Design Sensitivity Analysis: Overview and Review, *Inverse Problems in Engineering*, 1, 71-105, 1994.

[4] KH. Chew, K. Tai, E.Y.K. Ng, M. Muskulus, *Optimization of Offshore Wind Turbine Support Structures Using Analytical Gradient-Based Method*, Technical Report BAT/MB/OW-R01/2015, Norwegian University of Science and Technology, Trondheim, Norway, 23 pp, 2015.

[5] DNV, Fatigue Design of Offshore Steel Structures, Recommended Practice DNV-RP-C203, Det Norske Veritas AS, Høvik, Norway, 178 pp, 2012.

[6] IEC, *Wind Turbines – Part 1: Design Requirements*, International Standard IEC 61400:1, International Electrotechnical Commission, Geneva, Switzerland, 85 pp, 2005.

[7] IEC, *Wind Turbines – Part 3: Design Requirements for Offshore Wind Turbines*, International Standard IEC 61400:3, International Electrotechnical Commission, Geneva, Switzerland, 263 pp, 2009.

[8] ASTM, *Standard Practices for Cycle Counting in Fatigue Analysis*, ASTM E1049-85, American Society of Testing Materials, West Conshohocken, USA, 10 pp, 2011.

[9] T. Dirlik, *Application of Computers in Fatigue Analysis*, PhD Thesis, Univ of Warwick, UK, 234 pp, 1985.

[10] G.J. Park, *Analytic Methods for Design Practice*, Springer, Berlin, 627 pp, 2007.

[11] P. Ragan and L. Manuel, Comparing Estimates of Wind Turbine Fatigue Loads using Time-Domain and Spectral Methods, *Wind Engineering*, 31 (2), 83-99, 2007.

[12] J. Jonkman, S. Butterfield, W. Musial and G. Scott, *Definition of a 5MW Reference Wind Turbine for Offshore System Development*, Technical Report NREL/TP-500-38060, National Renewable Energy Laboratory, Golden, CO, 63 pp, 2009.

[13] F. Vorpahl, W. Popko and D. Kaufer, *Description of a Basic Model of the "UpWind Reference Jacket" for Code Comparison in the OC4 Project under IEA Wind Annex*, Technical Report, Fraunhofer IWES, Bremerhaven, 14 pp, 2011.